

Spectroscopy of Dark Soliton States in Bose-Einstein Condensates

K. Bongs[†], S. Burger[‡], D. Hellweg[§], M. Kottke[§], S. Dettmer[§],
T. Rinkleff[§], L. Cacciapuoti[§], J. Arlt[§], K. Sengstock[†] and W.
Ertmer[§]

[†] Institut für Laserphysik, Universität Hamburg, Jungiusstr. 9, 20355 Hamburg, Germany

[‡] LENS, Dipartimento di Fisica, Università di Firenze and Istituto Nazionale per la Fisica della Materia, Largo E. Fermi 2, I-50125 Firenze, Italy

[§] Institut für Quantenoptik, Universität Hannover, Welfengarten1, 30167 Hannover, Germany

E-mail: kai.bongs@physnet.uni-hamburg.de

Abstract. Experimental and numerical studies of the velocity field of dark solitons in Bose-Einstein condensates are presented. The formation process after phase imprinting as well as the propagation of the emerging soliton are investigated using spatially resolved Bragg-spectroscopy of soliton states in Bose-Einstein condensates of ⁸⁷Rubidium. A comparison of experimental data to results from numerical simulations of the Gross-Pitaevskii equation clearly identifies the flux underlying a dark soliton propagating in a Bose-Einstein condensate. The results allow further optimization of the phase imprinting method for creating collective excitations of Bose-Einstein condensates.

PACS numbers: 03.75.Fi, 32.80.Pj, 03.75.-b

Submitted to: *J. Opt. B: Quantum Semiclass. Opt.*

1. Introduction

With the realization of Bose-Einstein condensation (BEC) in dilute atomic gases [1, 2, 3], a well controllable and easily observable macroscopic wavefunction has become accessible for a wide variety of fundamental experiments. Since the early experiments on oscillations of the condensate [4, 5] and phonons [6], excitations of the condensate wavefunction have been subject to intense investigation. Signatures of superfluidity in Bose-Einstein condensates were first observed in the suppression of excitations below a critical excitation velocity [7, 8] and in the analysis of scissors mode excitations [9]. Recently another striking aspect of superfluidity in BEC has been studied by exciting vortices in two-component condensates [10] and vortices and vortex arrays in stirred condensates [11, 12, 13, 14, 15, 16]. Vortices as topological excitations of the condensate wavefunction represent particularly interesting phenomena and are still a very active area of research. Dark solitons in Bose-Einstein condensates are in several respects the one-dimensional counterpart to vortices. While the phase of the vortex wavefunction winds up around a zero density 'core', in a dark soliton state regions of constant phase are separated by a minimum in density and a steep phase gradient. Dark solitons are fundamental excitations in one dimensional systems described by nonlinear wave equations and thus a solution of the Gross Pitaevskii equation, which describes the condensate wave function [17]. In Bose-Einstein condensates, the creation of dark solitons using a phase imprinting method [18] has been investigated in a strongly elongated geometry in BECs of ^{87}Rb [19] and in nearly spherical BECs of ^{23}Na [20]. Recently bright solitons in Bose-Einstein condensates with attractive interactions [21, 22] and filled solitons [23] have also been observed .

The experiments on dark solitons have so far concentrated on the temporal evolution of the density distribution of the Bose-Einstein condensate, which showed the motion and decay of these excitations. In this article we extend these investigations to the velocity field which underlies a dark soliton state in a Bose-Einstein condensate.

2. Properties of dark solitons

In general Solitons are fundamental wave-packet-like excitations of one dimensional nonlinear systems. One characteristic of them is that they do not disperse but preserve their shape due to a balance between dispersive and stabilizing effects in these systems. Dark solitons in Bose-Einstein condensates form density minima, which self stabilize due to a balance of the repulsive mean field interaction which would be minimized by compressing the minimum and quantum pressure. The quantum pressure is related to the kinetic energy associated with the dark soliton velocity field, which is minimized by widening the minimum.

More formally a dark soliton in a homogeneous Bose-Einstein condensate of density

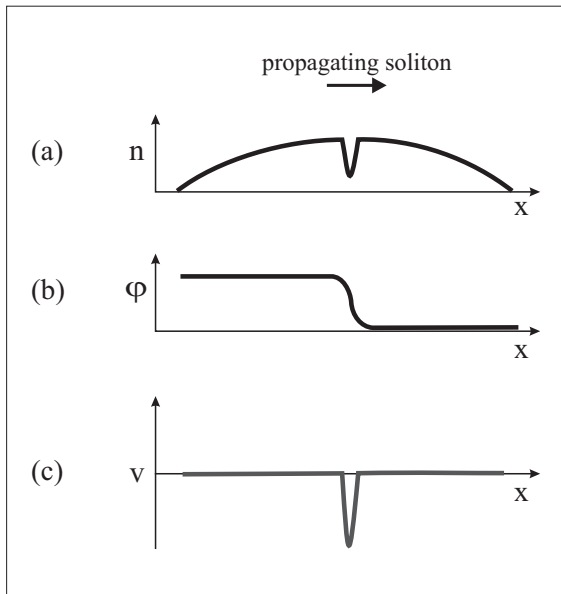


Figure 1. Schematic of the density distribution (a), phase distribution (b), and the resulting velocity distribution (c) of a dark soliton propagating in a BEC.

n_0 is described by the one dimensional wavefunction [24]

$$\Psi_k(x) = \sqrt{n_0} \left(i \frac{v_k}{c_s} + \sqrt{1 - \frac{v_k^2}{c_s^2}} \tanh \left[\frac{x - x_k}{l_0} \sqrt{1 - \frac{v_k^2}{c_s^2}} \right] \right), \quad (1)$$

with the position x_k and velocity v_k of the dark soliton, the correlation length $l_0 = (4\pi a n_0)^{-1/2}$, and the speed of sound $c_s = \sqrt{4\pi a n_0 \hbar} / m$, where m is the atom mass. Note that a so called black soliton with zero density at the minimum and a π phase jump is obtained for $v_k = 0$, while for all other cases the condensate wave function has nonzero amplitude at the position of the density minimum which now moves along the condensate and is associated with a finite phase gradient.

Consequently dark solitons in Bose-Einstein condensates are density minima associated with a steep phase gradient of the condensate wavefunction. This gradient of the phase distribution $\Phi(\vec{r})$ of the macroscopic Bose-Einstein condensate wavefunction defines a probability current density, which can be interpreted as a superfluid velocity field $v(\vec{r}) = \frac{\hbar}{m} \nabla \Phi(\vec{r})$. Thus, the steep gradient of the phase at the dark soliton leads to a localized peak in the velocity distribution of the BEC. The corresponding BEC density, phase and velocity distributions are shown schematically in Fig. 1.

Equation 1 is strictly valid only for infinite homogeneous one-dimensional systems but many qualitative features remain valid in more realistic experimental cases. However the effect of the trapping potential, the formation process and the dynamics during time-of-flight expansion are not included. In order to model these cases more accurately, we numerically solve the Gross-Pitaevski equation for the case of inhomogeneous

condensates, trapped in static potentials. Deviations from the 1D behaviour in elongated and nearly spherical traps are treated e.g. in [25, 26, 27].

3. Creation of dark solitons

For the experimental investigation of the dark soliton velocity field we first produce ground state Bose-Einstein condensates of ^{87}Rb as described in [28]. The condensates typically contain 1.5×10^5 atoms in the ($F=2$, $m_F=+2$) state, with less than 10% of the atoms being in the thermal cloud. The fundamental frequencies of our static magnetic trap are $\omega_x = 2\pi \times 14 \text{ Hz}$ and $\omega_\perp = 2\pi \times 425 \text{ Hz}$ along the axial and radial directions. The condensates are cigar-shaped with the long axis (x -axis) oriented horizontally and an aspect ratio of $\lambda \approx 30$, providing an essentially one dimensional potential for the evolution of the dark soliton on the time scale of the experiment.

In our experimental setup we create dark solitons using a phase imprinting method [18, 19]. The phase distribution of the condensate is changed by using the dipole potential of a far detuned light field ($\lambda = 532 \text{ nm}$, $I \approx 20 \text{ W/mm}^2$), illuminating one half of the condensate for a time t_p on the order of $20 \mu\text{s}$. Note that this time has to be shorter than the correlation time of the condensate, $t_c = \hbar/\mu$, in order to obtain pure phase imprinting, where μ is the chemical potential and in our case $t_c \approx 55 \mu\text{s}$. This procedure creates a moving dark soliton and a counterpropagating density wave, which become well separated after some time, t_{ev} , of further nonlinear evolution in the trapped Bose-Einstein condensate, as shown in Fig. 2 a).

Figure 2 b) shows a typical density-distribution of a dark soliton state created by phase imprinting after some evolution time in a trapped BEC obtained by the numerical solution of the GPE in 1D using the split operator method [19]. This simulation contains a finite optical resolution for the phase imprinting field, leading to a potential gradient with a width of $2 \mu\text{m}$ at the edge of the illuminated area, as realized experimentally. Due to this gradient a density wave and some higher order excitations moving to the right are created in addition to the dark soliton. The dark soliton and the density wave move in opposite directions, however the dark soliton is much narrower due to its self stabilization in the nonlinear medium. Note that the velocity field in the region of the dark soliton has only components of negative velocities, $v(x) < 0$ for a positive soliton velocity $v_k > 0$. This can be intuitively understood by the fact that a movement of the density minimum necessitates a transfer of matter in the opposite direction.

4. Bragg spectroscopy

Bragg diffraction has been used as a tool to manipulate Bose-Einstein condensates [29] in a number of experiments. It was used to evaluate the velocity distribution of a BEC within the magnetic trap and during time-of-flight experiments [30]. It has also served as a beam-splitter in an interferometer [31], for interferometric studies of the phase evolution of BECs [32] and even as an outcoupling mechanism for an atom laser

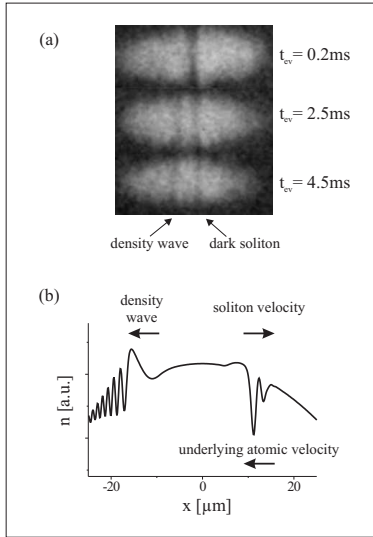


Figure 2. a) Absorption images of Bose-Einstein condensates which evolved in the magnetic trap for a time, t_{ev} after phase imprinting. The images were taken after an additional time-of-flight of 4 ms, leading to density minima for the dark soliton as well as for a density wave [19]. b) Numerical simulation of the density distribution of a dark soliton propagating in a BEC. The density data shown was obtained for the same parameters as used for the velocity field in Fig. 6.

[33]. In addition Bragg diffraction was employed as a tool for the realization of exciting experiments on non-linear effects in BECs [34] and their possible application to create entanglement [35]. However, a complete review of the use of Bragg spectroscopy in experiments on BEC is beyond the scope of this paper.

Fig. 3 schematically shows the Bragg diffraction process used in the experiments described here (a more detailed explanation can be found in [29]). Two counterpropagating laser beams induce a two photon transition between two momentum states which differ by two photon momenta, $2\hbar k$. Thus the atoms which have been in resonance with the Bragg-transition will be separated from the remaining atoms by $\Delta x = \frac{2\hbar k t_{\text{tof}}}{m}$, where t_{tof} is the time-of-flight after the Bragg pulse. Since the resonance condition depends on the initial velocity of the atom, a given difference frequency of the laser beams addresses a specific velocity class within the condensate. The width of this resonance corresponds to the Fourier transform of the applied laser pulse envelope. For ^{87}Rb and counterpropagating laser beams the velocity dependence of the resonance condition is given by $\frac{\Delta v}{\delta/2\pi} \approx 0.39 \frac{\text{mm/s}}{\text{kHz}}$.

Experiments employing Bragg diffraction on BEC can be divided in two general areas. By using short, intense pulses all velocity classes within a BEC can be accessed and transferred into a moving state. This process corresponds to a variable, coherent beamsplitter for matterwaves. On the other hand, long pulses are selective to the

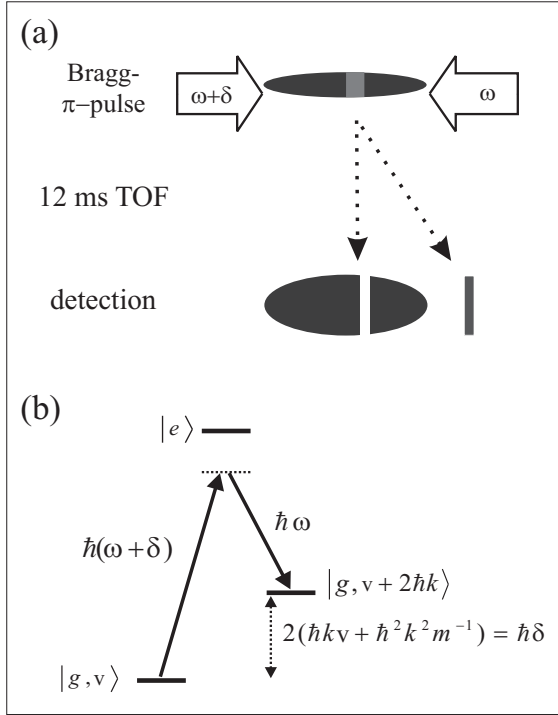


Figure 3. a) Schematic of position resolved Bragg-spectroscopy of a dark soliton state in a BEC. b) Energy level scheme for the Bragg transition between ground state levels with velocities v and $v + \frac{2\hbar k}{m}$ where k is the wave number of the laser field. The resonance condition for a given frequency difference δ is only fulfilled for a certain velocity v .

velocity in the BEC and distinct velocity classes can be addressed. This process is used to examine the flux underlying dark solitons in Bose-Einstein condensates. We show that it is also possible to extract spatially resolved information from these measurements, rather than only counting the outcoupled number of atoms.

The experimental sequence starts with the creation of a Bose-Einstein condensate in the magnetic trap followed by phase imprinting for the creation of the soliton (as discussed above). After phase imprinting the condensate evolves in the magnetic trap for a time t_{ev} which is varied in order to observe the soliton excitation during formation and later propagation. The Bragg scattering takes place after switching off the magnetic trapping potential. For the experiments a free expansion time, $t_{exp} = 2$ ms, is used after release from the trap in order to reduce the atomic density before applying the Bragg pulse. Collisions between atoms in different Bragg orders are thus negligible. In order to suppress spontaneous processes the frequencies of the Bragg lasers are detuned from the transition $|F = 2\rangle \rightarrow |F'\rangle$ by 6.8 GHz. The Bragg pulse is usually applied for a duration of $t_{Bragg} = 250 \mu s$, and a time-of-flight of $t_{TOF} = 13$ ms after the pulse is used before detection ($t_{Bragg} = 500 \mu s$ and $t_{TOF} = 11$ ms for the BEC spectroscopy in Fig.

7).

5. Velocity selective spectroscopy

The velocity selective Bragg scattering process described above is a widely applicable tool to investigate the behaviour of Bose-Einstein condensates. In the following we first observe the formation process of dark solitons due to the phase imprinting method. This is achieved by monitoring the spatial velocity almost immediately after the phase has been imprinted. In a second set of experiments the soliton is observed after a longer evolution time, t_{ev} , in the magnetic trap, in order to investigate the associated matter flux.

5.1. Soliton formation

Fig. 4 shows absorption images of atomic clouds after the above Bragg spectroscopy scheme has been applied with $t_{ev} = 0.2$ ms and different resonance conditions. The upper image (i) was obtained for an off-resonant Bragg pulse and thus just corresponds to a time-of-flight image of the BEC after phase imprinting. Image (ii) shows the case of a Bragg pulse resonant with the resting atoms, which thus obtain a velocity, $2\hbar k$, and appear to the right of their position in image (i) due to their horizontal movement during the time-of-flight period of 13 ms after phase imprinting. The moving atoms within the cloud are not resonant with the Bragg pulse and remain on the left. They correspond to the density wave and dark soliton. The velocity of these atoms can be determined to be negative, as expected, by scanning the Bragg frequency difference. The density distributions corresponding to Bragg scattering resonant with negative velocity atoms are shown in image (iii), with the resting atoms on the left and the moving atoms on the right.

The simulations show that the velocity field in the Bose-Einstein condensate after the short evolution time, $t_{ev} = 0.2$ ms corresponds almost exclusively to the velocity field induced by the phase imprinting pulse. Fig. 5 shows calculated density and phase distributions in the magnetic trap for various times after the phase imprinting pulse. At $t_{ev} = 0$ there is no density change but only a phase gradient in the center of the condensate, which corresponds to a velocity field. The associated flow quickly leads to the formation of a density maximum, moving to the left and a density minimum moving to the right. These two start to separate after approximately $t_{ev} = 0.5$ ms with a subsequent dispersive spreading of the density maximum and a narrowing of the density minimum which leads to the dark soliton state. Note that the initial phase gradient is split between the density wave and the dark soliton since both are associated with some flow of matter.

The evolution of the wavefunction in Fig. 5 clearly shows that the mechanism of phase imprinting with finite resolution relies on the joint action of a phase shift and a local removal of atoms due to a momentum transfer. The momentum imparted on some

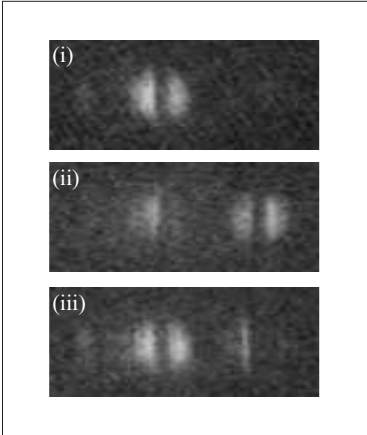


Figure 4. a) Absorption images for different detunings δ of the Bragg-pulses: (i) off-resonant, (ii) resonant with velocities $v = 0$, (iii) resonant with velocities $v < 0$. These images were obtained for a short evolution time in the magnetic trap of $t_{ev} = 0.2$ ms.

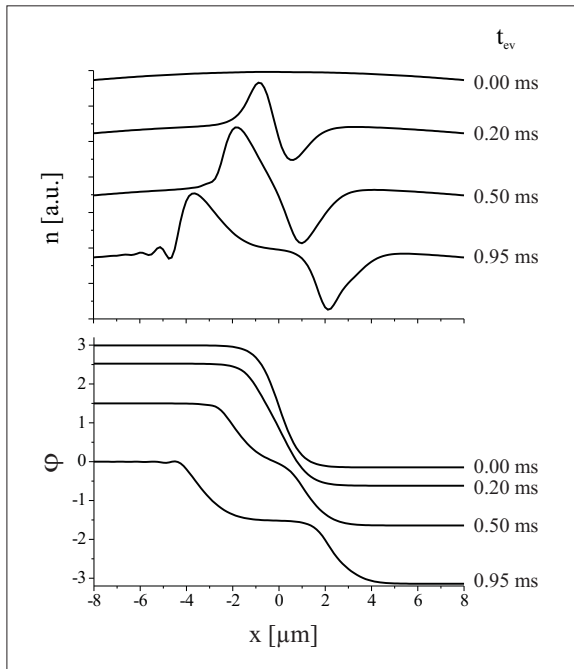


Figure 5. Density and phase of the condensate wavefunction from numerical solutions of the Gross Pitaevskii equation for short evolution times in the magnetic trap after phase imprinting. For these simulations the width of the light field edge was assumed to be $2\mu\text{m}$. These simulations show that for the experimental parameters the soliton and density wave are not yet distinguishable. Note that in this case the simulation only shows the central part of the condensate and doesn't include any time of flight.

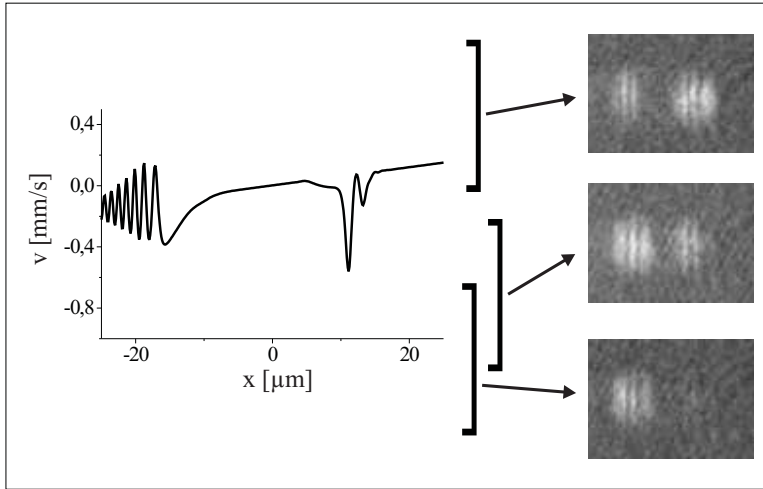


Figure 6. Left: velocity distribution of a dark soliton state after phase imprinting with a phase difference $\Delta\phi = \pi$, an evolution time in the magnetic trap $t_{ev} = 3.5$ ms, and $t_{TOF} = 2$ ms of time of flight from a numerical simulation of the Gross-Pitaevskii equation. Right: corresponding Bragg spectroscopy images for different resonance conditions of $v = +0.5$ mm/s, $v = -0.7$ mm/s and $v = -1.1$ mm/s (from top to bottom). The height of the vertical bars indicates the width of the Bragg resonance, thus representing the velocity classes, which will be scattered during the Bragg pulse.

parts of the wave function, assists in the later formation of a dark soliton due to the removal of density from the region of the soliton. The images in Fig. 4 confirm these numerical results. The imparted momentum can be explained classically by the finite width of the edge of the phase imprinting field, which produces a classical force due to the gradient of the light induced AC-Stark shift potential.

5.2. Flux associated with a dark soliton

At short evolution times the dark soliton is masked by other excitations induced by the phase imprinting pulse, but after a few ms it becomes apparent due to its self stabilization and slow propagation. An evolution time of $t_{ev} = 3.5$ ms is sufficient to fully separate the soliton and the density wave as shown by the Bragg scattering experiments and the numerical simulation in Fig. 6.

From the numerical simulation one expects to find local negative velocity components around $v \approx -0.5$ m/s at the positions of the density wave as well as of the dark soliton. The top right image shows nearly resting atoms scattered to the right, while two distinct lines of moving atoms remain on the left: the atoms associated with the dark soliton and the density wave. This scattering behaviour is inverted for a

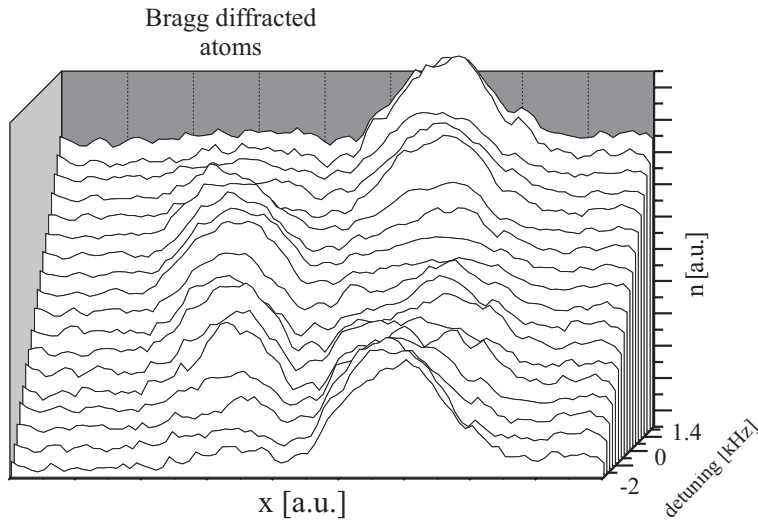


Figure 7. Vertically summed cuts through Bragg spectroscopy images of a Bose-Einstein condensate without phase imprinting. The Bragg pulse duration for this data was $500 \mu\text{s}$. The Bragg resonance frequency is changed by 200 Hz (corresponding to $\Delta v \approx 0.08 \text{ mm/s}$) between subsequent cuts. (Note that for technical reasons the position of the scattered atoms is on the other side as for the other images.)

negative velocity Bragg resonance, now scattering the two lines to the right and leaving the resting atoms on the left. No atom is effected by a Bragg pulse resonant with larger negative velocities in the bottom image, showing the limited range of the velocity field in the matter wave. This is clear evidence of the matter wave flux associated with a moving dark soliton.

6. Mapping the velocity field

In addition to the above examples of Bragg scattering for a few distinct resonance velocities, which clearly show the signature of dark soliton excitations, we use this method to fully map the underlying velocity field.

We first explain and verify the scheme by mapping the spatial velocity distribution of a pure Bose-Einstein condensate before applying it to a dark soliton excitation. The starting point is a systematic series of Bragg scattering data of a Bose-Einstein condensate after 2 ms of time of flight, as shown in Fig. 7. By taking a vertical cut through the data sets in the region of the scattered peak one obtains the amount of scattered atoms at a fixed position as a function of Bragg detuning. The maximum of this distribution then directly leads to the mean velocity of the atoms scattered to this position. Their original position in the condensate is then retrieved by accounting for their time-of-flight displacement due to the imparted momentum and their original

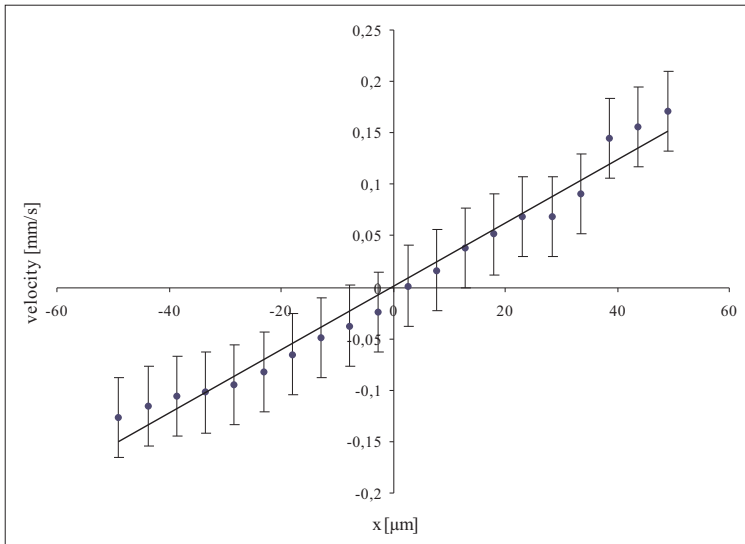


Figure 8. Velocity field of a freely falling Bose-Einstein condensate as determined from the series of Bragg scattering data in Fig. 7.

velocity. Repeating this procedure for the position range of the scattered peak this procedure directly gives the velocity field of the condensate wavefunction. In addition to analyzing the scattered peak, we cross check the velocity field data by generating the same data from the inverse behaviour of the non-scattered cloud.

Fig. 8 shows the extracted velocity as a function of position in the Bose condensate. The result is fitted with a linear velocity distribution according to the expected behaviour in the Thomas-Fermi limit. The good agreement confirms the validity of this analysis.

By applying the above method to the dark soliton excitation discussed in section 5.2 we find the underlying velocity field as shown in Fig. 9.

The comparison of the experimental data to the theoretical curve shows good agreement within the finite experimental resolution, which demonstrates the applicability of position resolved Bragg spectroscopy to the investigation of excitations in Bose-Einstein condensates.

7. Conclusions

In conclusion we have investigated the matter wave dynamics due to phase imprinting and the matter wave flux underlying a moving dark soliton. Both experiments and theoretical predictions clearly show that the dark soliton movement is associated with a particle flux in the opposite direction. It was demonstrated that Bragg diffraction methods can be used to analyse the spatial phase and the density distribution of dark soliton states in Bose-Einstein condensates.

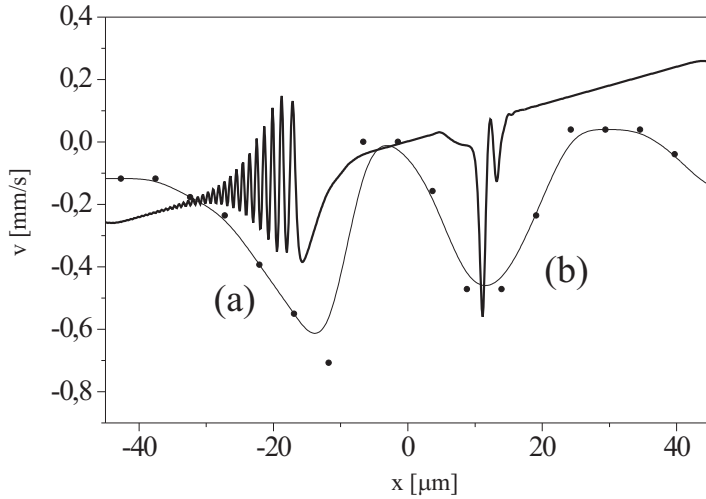


Figure 9. Velocity field underlying the dark soliton excitation in section 5.2 in comparison to the numerical simulation from Fig. 6. The fit through the experimental data is a spline fit to guide the eye. The negative velocity peaks (a) and (b) correspond to the density wave and the dark soliton respectively. Note that the averaging effect of the experimental data is mainly due to the finite optical resolution of $\approx 15 \mu\text{m}$ used for this set of measurements.

Future improvements of the tool of the position resolved Bragg spectroscopy technique rely on the use of longer pulses and higher resolution in the detection system. This should allow for precision measurements on many kinds of excitations in Bose-Einstein condensates. In this respect the investigation of the interplay between the imprinted phase and the associated imparted momentum promises important advances in the creation and study of excitations in Bose-Einstein condensates.

Acknowledgments

We gratefully acknowledge Anna Sanpera for help with the numerical simulations and thank the DFG for support in the Sonderforschungsbereich 407 as well as the European Union for support in the RTN network "Preparation and application of quantum-degenerate cold atomic/molecular gases" contract no: HPRN-CT-2000-00125.

- [1] M.H. Anderson, J.R. Ensher, M.R. Matthews, C.E. Wieman, and E.A. Cornell 1995 Observation of Bose-Einstein condensation in a dilute atomic vapor *Science* **269** 198
- [2] K.B. Davis, M.-O. Mewes, M.R. Andrews, N.J. van Druten, D.S. Durfee, D.M. Kurn, and W. Ketterle 1995 Bose-Einstein condensation in a gas of sodium atoms *Phys. Rev. Lett.* **75** 3969
- [3] C.C. Bradley, C.A. Sackett, J.J. Tollett, and R.G. Hulet 1995 Evidence of Bose-Einstein

- condensation in an atomic gas with attractive interactions *Phys. Rev. Lett.* **75** 1687 *ibid.* 1997 **79** 1170
- [4] D.S. Jin, J.R. Ensher, M.R. Matthews, C.E. Wieman, and E.A. Cornell 1996 Collective excitations of a Bose-Einstein condensate in a dilute gas *Phys. Rev. Lett.*, **77** 420
- [5] M.-O. Mewes, M.R. Andrews, N.J. van Druten, D.M. Kurn, D.S. Durfee, C.G. Townsend, and W. Ketterle 1996 Collective excitations of a Bose-Einstein condensate in a magnetic trap *Phys. Rev. Lett.* **77** 988
- [6] M.R. Andrews, D.M. Kurn, H.-J. Miesner, D.S. Durfee, C.G. Townsend, S. Inouye, and W. Ketterle 1997 Propagation of sound in a Bose-Einstein condensate *Phys. Rev. Lett.* **79** 553 *ibid.* 1998 **80** 2967
- [7] C. Raman, M. Köhl, R. Onofrio, D.S. Durfee, C.E. Kuklewicz, Z. Hadzibabic, and W. Ketterle 1999 Evidence for a critical velocity in a Bose-Einstein condensed gas *Phys. Rev. Lett.* **83** 2502
- [8] R. Onofrio, C. Raman, J.M. Vogels, J.R. Abo-Shaeer, A.P. Chikkatur, and W. Ketterle 2000 Observation of superfluid flow in a Bose-Einstein condensed gas *Phys. Rev. Lett.* **85** 2228
- [9] O.M. Maragó, S.A. Hopkins, J. Arlt, E. Hodby, G. Heckenblaikner, and C.J. Foot 2000 Observation of the scissors mode and evidence for superfluidity of a trapped Bose-Einstein condensed gas *Phys. Rev. Lett.* **84** 2056
- [10] M.R. Matthews, B.P. Anderson, P.C. Haljan, D.S. Hall, C.E. Wieman, and E.A. Cornell 1999 Vortices in a Bose-Einstein Condensate *Phys. Rev. Lett.* **83** 2498
- [11] K.W. Madison, F. Chevy, W. Wohlleben, and J. Dalibard 2000 Vortex formation in a stirred Bose-Einstein condensate *Phys. Rev. Lett.* **84** 806
- [12] F. Chevy, K.W. Madison, and J. Dalibard 2000 Measurement of the angular momentum of a rotating Bose-Einstein condensate *Phys. Rev. Lett.* **85** 2223
- [13] E. Hodby, G. Heckenblaikner, S.A. Hopkins, O.M. Maragó, and C.J. Foot 2001 Vortex nucleation in Bose-Einstein condensates in an oblate, purely magnetic potential *Phys. Rev. Lett.* **88** 010405
- [14] S. Inouye, S. Gupta, T. Rosenband, A.P. Chikkatur, A. Görlitz, T.L. Gustavson, A.E. Leanhardt, D.E. Pritchard, and W. Ketterle 2001 Observation of vortex phase singularities in Bose-Einstein condensates *Phys. Rev. Lett.* **87** 080402
- [15] J.R. Abo-Shaeer, C. Raman, J.M. Vogels, and W. Ketterle 2001 Observation of vortex lattices in Bose-Einstein condensates *Science* **292** 476
- [16] P.C. Haljan, I. Coddington, P. Engels, and E.A. Cornell 2001 Driving Bose-Einstein-condensate vorticity with a rotating normal cloud *Phys. Rev. Lett.* **87** 210403
- [17] L.P. Pitaevskii 1961 Vortex lines in an imperfect Bose gas *Sov. Phys. JETP* **13** 451
- [18] L. Dobrek, M. Gajda, Maciej Lewenstein, K. Sengstock, G. Birkl, and W. Ertmer 1999 Optical generation of vortices in trapped Bose-Einstein condensates *Phys. Rev. A* **60** R3381
- [19] S. Burger, K. Bongs, S. Dettmer, W. Ertmer, K. Sengstock, A. Sanpera, G.V. Shlyapnikov, and M. Lewenstein 1999 Dark solitons in Bose-Einstein condensates *Phys. Rev. Lett.* **83** 5198
- [20] J. Denschlag, J.E. Simsarian, D.L. Feder, Charles W. Clark, L.A. Collins, J. Cubizolles, L. Deng, E.W. Hagley, K. Helmerson, W.P. Reinhardt, S.L. Rolston, B.I. Schneider, and W.D. Phillips 2000 Generating solitons by phase engineering of a Bose-Einstein condensate *Science* **287** 97
- [21] L. Khaykovich, F. Schreck, G. Ferrari, T. Bourdel, J. Cubizolles, L. D. Carr, Y. Castin, and C. Salomon 2002 Formation of a matter-wave bright soliton *Science* **296** 1290
- [22] Kevin E. Strecker, Guthrie B. Partridge, Andrew G. Truscott, and Randall G. Hulet 2002 Formation and propagation of matter-wave soliton trains *Nature* **417** 150
- [23] B.P. Anderson, P.C. Haljan, C.A. Regal, D.L. Feder, L.A. Collins, C.W. Clark, and E.A. Cornell 2001 Watching dark solitons decay into vortex rings in a Bose-Einstein condensate *Phys. Rev. Lett.* **86** 2926
- [24] P.O. Fedichev, A.E. Muryshev, and G. V. Shlyapnikov 1999 Dissipative dynamics of a kink state in a Bose-condensed gas *Phys. Rev. A* **60** 3220
- [25] A. E. Muryshev, H. B.V. van den Heuvel, and G.V. Shlyapnikov 1999 Stability of standing matter waves in a trap *Phys. Rev. A* **60** R2665

- [26] D. L. Feder, M. S. Pindzola, L. A. Collins, B. I. Schneider, and C. W. Clark 2000 Dark-soliton states of Bose-Einstein condensates in anisotropic traps *Phys. Rev. A* **62** 053606
- [27] A. Muryshv, G. V. Shlyapnikov, W. Ertmer, K. Sengstock, and M. Lewenstein 2002 Dynamics of Dark Solitons in Elongated Bose-Einstein Condensates *Phys. Rev. Lett.* **89** 110401
- [28] K. Bongs, S. Burger, G. Birkl, K. Sengstock, W. Ertmer, K. Rzażewski, A. Sanpera, and M. Lewenstein 1999 Coherent evolution of bouncing Bose-Einstein condensates *Phys. Rev. Lett.*, **83**, 3577
- [29] M. Kozuma, L. Deng, E.W. Hagley, J. Wen, R. Lutwak, K. Helmerson, S.L. Rolston, and W.D. Phillips 1999 Coherent splitting of Bose-Einstein condensed atoms with optically induced Bragg diffraction *Phys. Rev. Lett.* **82**, 871
- [30] J. Stenger, S. Inouye, A.P. Chikkatur, D.M. Stamper-Kurn, D.E. Pritchard, and W. Ketterle 1999 Bragg spectroscopy of a Bose-Einstein condensate *Phys. Rev. Lett.* **82**, 4569
- [31] Yoshio Torii, Yoichi Suzuki, Mikio Kozuma, Toshiaki Sugiura, Takahiro Kuga, Lu Deng, and E.W. Hagley 2000 Mach-Zehnder Bragg interferometer for a Bose-Einstein condensate *Phys. Rev. A* **61**,041602
- [32] J.E. Simsarian, J. Denschlag, Mark Edwards, Charles W. Clark, L. Deng, E.W. Hagley, K. Helmerson, S.L. Rolston, and W.D. Phillips 2000 Imaging the phase of an evolving Bose-Einstein condensate wave function *Phys. Rev. Lett.* **85** 2040
- [33] E.W. Hagley, L. Deng, M. Kozuma, J. Wen, K. Helmerson, S.L. Rolston, and W.D. Phillips 1999 A well-collimated quasi-continuous atom laser *Science* **283** 1706
- [34] L. Deng, E.W. Hagley, J. Wen, M. Trippenbach, Y. Band, P.S. Julienne, J.E. Simsarian, K. Helmerson, S.L. Rolston, and W.D. Phillips 1999 Four-wave mixing with matter waves *Nature* **398** 218
- [35] J.M. Vogels, K. Xu, and W. Ketterle 2002 Generation of macroscopic pair-correlated atomic beams by four-wave mixing in Bose-Einstein condensates *Phys. Rev. Lett.* **89** 020401